Atmospheric dispersion compensation for extremely large telescopes

Alexander V. Goncharov, Nicholas Devaney, and Christopher Dainty

Department of Experimental Physics, National University of Ireland, Galway, Ireland
alexander.goncharov@nuigalway.ie, nicholas.devaney@nuigalway.ie, c.dainty@nuigalway.ie

Abstract: Achieving diffraction limited imaging with future ground-based optical telescopes will require adaptive optics for correction of atmospheric turbulence and also efficient techniques for atmospheric dispersion compensation. We study the benefit of using a linear atmospheric dispersion corrector (ADC) coupled with a deformable mirror on a 42-m Extremely Large Telescope (ELT) operating in the VIRJ spectral bands. The ADC design consists of two identical thin wedges made of F5 glass. The amount of dispersion introduced by the ADC is adjusted by translating one of the wedges along the optical axis so that it always cancels atmospheric dispersion as it varies with telescope elevation. We show that the ADC working in conjunction with a deformable mirror provides diffraction-limited image quality over a 1-arcmin field.

©2007 Optical Society of America

OCIS codes: (110.6770) Telescopes, (220.1000) Aberration compensation, (010) Atmospheric propagation (010.1300), Adaptive optics (010.1080).

References and links

1. F. Roddier, "The effects of atmospheric turbulence in optical astronomy," in E. Wolf, ed., *Progress in Optics* (North-Holland, Amsterdam, 1981), Vol. **19**, pp. 341-350.
2. R. A. Gonsalves, "Compensation of scintillation with a phase-only adaptive optic," Opt. Lett. **22**, 588-590 (1997).
3. J. D. Barchers, "Closed-loop stable control of two deformable mirrors for compensation of amplitude and phase fluctuations," J. Opt. Soc. Am. A **19**, 926-945 (2002)
4. A. A. Tokovinin, "Polychromatic scintillation," J. Opt. Soc. Am. A **20**, 686-689 (2003).
5. C.B. Hogge & R.R. Butts, "Effects of using different wavelengths in wave-front sensing and correction," J. Opt. Soc. Am. **72**, 606-609 (1982).
6. N. Devaney, Applied Optics Group, National University of Ireland, Galway, Ireland, is preparing a manuscript to be called "The chromatic effects of the atmosphere in astronomical adaptive optics."
7. E. P. Wallner, "The effects of atmospheric refraction on compensated imaging," Proc. SPIE **75**, 119-125 (1976).
8. E. P. Wallner, "Minimizing atmospheric dispersion effects in compensated imaging," J. Opt. Soc. Am. **67**, 407-409, (1977).
9. E. P. Wallner, "Comparison of diffractive and refractive effects in two-wavelength adaptive transmission," J. Opt. Soc. Am. A **1**, 785-787 (1984).
10. J. W. Hardy, Adaptive Optics for Astronomical Telescopes (Oxford U. Press, 1998).
11. J. C. Owens, "Optical refractive index of air: dependence on pressure, temperature and composition," Appl. Opt. **6**, 51-59 (1967).
12. P. E. Ciddor, "Refractive index of air: new equations for the visible and near infrared," Appl. Opt. **35**, 1566-1573 (1996).
13. M. Owner-Petersen and A Goncharov, "Some consequences of Atmospheric Dispoersion for ELTs," *Proc.* SPIE **5489,** 526-531 (2004).
14. N. S. Nightingale and D. F. Buscher, "Interferometric seeing measurements at the La Palma Observatory," Mon. Not. R. Astron. Soc. **251**, 155–166 (1991)
15. M. M. Colavita, M. Shao, and D. H. Staelin, "Atmospheric phase measurements with the Mark III stellar interferometer," Appl. Opt. **26**, 4106–4112 (1987).
16. A. Ziad. M. Schöck, G. Chanan, M. Troy, R. Dekany, B. F. Lane, J. Borgnino, F. Martin, "Comparison of measurements of the outer scale of turbulence by three different techniques," Appl. Opt. **43**, 2316-2324 (2004).
17. R. J. Sasiela, "Wave-front correction by one or more synthetic beacons," J. Opt. Soc. Am. A **11**, 379-393 (1994).

18. M. Le Louarn and M. Tallon, "Analysis of modes and behavior of a multiconjugate adaptive optics system," J. Opt. Soc. Am. A **19**, 912-925 (2002).
19. C. G. Wynne and S. P. Worswick, "Atmospheric dispersion correctors at the Cassegrain focus," Mon. Not. R. Astron. Soc. **220**, 657-670 (1986).
20. C. G. Wynne "Correction of atmospheric dispersion in the infrared," Mon. Not. R. Astron. Soc. **282**, 863-867 (1996).
21. C. G. Wynne, "Atmospheric dispersion in very large telescopes with adaptive optics," Mon. Not. R. Astron. Soc. **285**, 130-134 (1997).
22. C. G. Wynne, "A new form of atmospheric dispersion corrector," Mon. Not. R. Astron. Soc. **262**, 741-748 (1993).
23. T. G. Haywarden, E. Attad, C. R. Cunningham, D. M. Henry, C. J. Norrie, M. Wells, C. J. Dainty, N. Devaney and A. V. Goncharov, "WP 11300: Atmospheric dispersion compensation," FP6 Extremely large telescope design study, Interim Report (2006).
24. G. Avila, G. Rupprecht and J. M. Beckers, "Atmospheric dispertion correcton for the FORS focal reducers at ESO VLT," Proc. SPIE **2871**, 1135-1143 (1996).
25. T. Andersen, A. Ardeberg and M. Owner-Petersen, Euro50. Design study of a 50 m Adaptive Optics Telescope, (Lund Observatory, 2003), pp. 147-153.
26. A. V. Goncharov, Extremely large telescopes. Optical design and wavefront correction, PhD dissertation, Lund Observatory (2003), ISBN 91-628-5607-3, pp. 143-151.
27. M. Owner-Petersen "Effects of atmospheric dispersion on the PSF background level," Proc. SPIE **6272,** 62722F-1 (2006).

1. Introduction

The Earth's atmosphere has various chromatic effects on light passing through it. Most of the optical effects are refractive and we shall consider their relevance for high resolution imaging with ground-based optical telescopes, but there is also a diffractive effect. This is due to the fact that a wave passing through a turbulent layer, having a random refractive index distribution, will undergo diffraction. Propagation of the wave will give rise to scintillation in the far field of the turbulent layer. This effect is well known [1] and accounts for a certain degradation of the performance attainable with an adaptive optics (AO) system that only corrects phase. In order to suppress amplitude variations (scintillation), an additional deformable mirror might be required [2, 3]. Since the angle through which light is diffracted depends on wavelength, the scintillation will be chromatic [4]. Hogge and Butts [5] examined the wavelength dependence on this effect, and found it to be severe if the wavelengths at which the wavefront phase error is sensed and corrected are widely separated. Assuming a Hufnagel-Valley turbulence profile, this effect is of order 2% reduction in Strehl ratio for wavefront sensing at 0.5 microns and correction at 1 micron [6]. It will become worse if the turbulence vertical profile contains strong, high-altitude layers. However, this effect depends very weakly on telescope diameter.

The refractive effects of the atmosphere may be divided into three types: (i) angular dispersion, (ii) chromatic path length error, and (iii) chromatic displacement error. These errors have been examined in some detail by Wallner in a series of publications [7-9]. They are summarised in the textbook on adaptive optics by Hardy [10]. Angular dispersion refers to the dependence of the apparent position of an astronomical object on wavelength, and it is due to the dispersion of air (differential refraction). The main topic of this paper is the correction of this effect with a compensating device. However, it should be noted that residual errors in angular dispersion correction become a concern when it is required to obtain high Strehl ratio at the diffraction limit of an ELT. The first concern is that the dispersion correcting device will be controlled according to an approximate model of atmospheric dispersion as a function of atmospheric pressure, temperature and relative humidity, and different formulae are available, with those of Owens [11] and Ciddor [12] being the most widely used. The accuracy of the Ciddor formula is $5 \ 10^{-8}$. Over the wavelength range 0.4 to 0.8 microns, this would give an error of 4 milliarcsec at a zenith distance of 45 degrees. The corresponding reduction in Strehl ratio would be severe. Uncertainties in atmospheric parameters would be a further source of error. Over the same bandwidth, the dependence is approximately 1.4 milliarcsec per K and 0.6 milliarcsec per millibar. Since these parameters can change rapidly, especially when weather conditions are unstable, it may be desirable to employ a dispersion

sensor and control the atmospheric dispersion corrector in real time rather than to rely on look-up tables alone.

Chromatic path length error arises simply because the optical path length depends on the refractive index of air, which is in turn wavelength dependent. A deformable mirror can correct perfectly at a single wavelength only. Wallner [9] derived a formula showing that this error is proportional to a factor multiplied by the uncorrected wavefront variance, and showed that the error is acceptable on a medium sized telescope. If the error is determined for an ELT it turns out to be so large that it would effectively limit AO on ELTs to narrow bandwidth observations. However, Owner-Petersen and Goncharov [13] showed that the error is greatly reduced if the outer scale of turbulence is comparable with the diameter of the telescope aperture. Measurements of the outer scale have given widely different values, from meters [14] to kilometres [15]. However, more recent measurements give typical values in the range 10-30m [16]. On a 50 m telescope with a 30 m outer scale, this effect would lead to a reduction of Strehl ratio of 4% at 0.9 microns if the wavefront sensing is carried out at 0.589 microns (Na laser wavelength) [6]. The outer scale is found to sometimes take on much larger values, and on these occasions there would be a reduction in AO performance over broad bands. Even for the outer scale comparable with telescope diameter the AO correction of wavefronts would be optimal only within one of the spectral bands, while for adjacent bands it would lead to over correction (at longer wavelengths) or under correction (at shorter wavelengths).

Dispersion displacement error is due to the fact that collimated white light after entering atmosphere is dispersed and laterally separated rays of different wavelengths in the vertical plane follow different paths through turbulence. The accumulated separation over a long propagation path results in lateral displacement of wavefronts of different colours at the telescope pupil. As with angular dispersion, the effect is zero if observing at zenith. For a broad bandwidth (0.4-0.9 microns) the effect would typically lead to a reduction in Strehl ratio of 3% at a zenith angle of 30 degrees [6]. It depends on the vertical distribution of turbulence, and does not depend on the telescope diameter.

2. Principle of the linear ADC

Operation conditions of an ELT dictate a particular configuration of the ADC optical design that is most suitable under a given set of constrains. As an example, we consider here an adaptive ELT featuring a 42-m ellipsoidal primary mirror (M1), which in conjunction with a 4-m concave ellipsoidal secondary mirror (M2) constitute an f/15.2 Aplanatic Gregorian (AG) system, which is shown in Fig. 1 together with a flat tertiary mirror M3 and a folding flat beamsplitter M4 delivering the final image onto a gravity stable Nasmyth platform.

This basic two-mirror AG configuration has several major functions. Ideally, it should provide a substantial (at least 0.5-1 arcmin) science field with near diffraction-limited image quality, which in practice will require the use of an adaptive secondary mirror and an atmospheric dispersion corrector (ADC). The AG system should also provide a somewhat larger (2-3 arcmin) unobstructed field for Laser Guide Star (LGS) path to ensure efficient AO system correction over the 1-arcmin science field using laser tomography [17, 18]. The light from LGSs passes through the beamsplitter M4, while the light from astronomical objects is reflected from M4 to the Nasmyth focus and corrected by the ADC.

Under such constraints, with a relatively slow F/15.2 converging beam, the minimum possible diameter of an ADC working near the Nasmyth focus exceeds 0.75 m. Due to the large optical diameter of the corrector we consider a linear ADC design as an alternative to a commonly used ADC systems with counter-rotating prisms [19, 20]. The latter concept is based on two zero-deviation prisms (two wedges of different glass each), which are jointly rotated against each other, and therefore the ADC becomes inherently thicker and more complicated compared to the two thin wedges of the linear ADC. Other solutions utilizing curved compound Amici prisms [21] or lens systems with a tipped monocentric meniscus about the common center of its outer surfaces [22] are not considered due to excessive curvature and thickness of the optical components. Performance analysis and a comparison of

different ADC designs working in relatively fast converging beams f/6 and f/13 for AO-corrected 50-m and 100-m ELTs have been presented in Ref. [23].
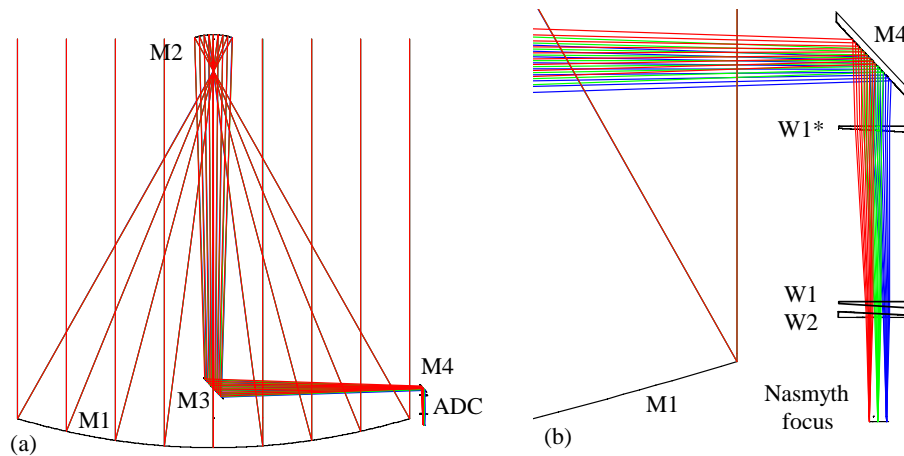

Fig. 1. Optical layout of a 42-m Aplanatic Gregorian telescope (a) with a linear ADC at the Nasmyth platform (b). W1* is the marginal position of the first wedge at 50 degrees off-zenith.

Originally, Beckers [24] suggested the concept of the linear ADC for the focal reducer and low dispersion spectrograph at two of the ESO 8-m telescopes. It has been adopted as a possible solution for atmospheric dispersion compensation on the Euro50 adaptive telescope [25, 26]. The underlying design principles, in particular the benefits of having an ELT with AO correction before the first well-corrected ELT focus, which is presented in the following and in section 3, have been conceive and developed in [25] and [26], including wavefront sensing schemes with LGSs. The optical design of a linear ADC for an f/13 Gregorian focus of a 50-m ELT has been also described in Ref. [23].

In contrast to the previous publications the present paper deals with the correction of atmospheric dispersion with a linear ADC in a slower f/15.2 beam at the Nasmyth focus of a reduced-aperture (42-m) ELT at larger Zenith angles (50 degrees). In particular, we do not use a tilt component of the secondary mirror when correcting variable intrinsic aberrations of the ADC, which greatly simplifies telescope alignment in view of the required field de-rotation at the Nasmyth focus. The field stabilization techniques to compensate the effect of the pupil displacement are outlined. We also present a more detailed analysis of the proper choice of wedge material in relation to the various spectral bands.

Figure 2(a) shows a schematic optical layout of the linear ADC and its dispersive effect on the propagation of rays of different colors. The ray bundles from an atmosphere-dispersed astronomical point source enter the telescope aperture, which is represented by a single lens L with focal length f. For clarity, we show only red and blue bundles of rays that form an angle ΔR, which corresponds to the differential refraction at these two wavelengths. The linear ADC consists of two identical wedges W1 and W2 with opposite orientation. The compensation of the atmosphere-induced spread of a point source into a spectrum at the focal plane F (approximately given by $\Delta R\, f$) is corrected by adjusting the axial separation of the wedges. The first wedge W1 introduces a large amount of dispersion of the opposite sign to the atmospheric dispersion. The second wedge W2 partly corrects for dispersion introduced by W1 and eliminates the telescope pupil tilt. The combined effect of the two wedges provides a small dispersion in the focal plane F. This small residual dispersion is due to mismatch between the dispersion of the atmosphere and the chosen glass material (secondary spectrum).

Figure 2(b) depicts the refractivity of air as a function of wavelength λ. It is evident that spectral bands B, V and R show rapid change of refractivity of air and hence the large amount of dispersion compared to I, J, H, K and thermal infrared bands. The B band is the most

challenging for atmospheric dispersion correction and also for AO correction, while the K band does not need an ADC corrector, and we therefore limit our design specifically to V, R, I, and J bands.
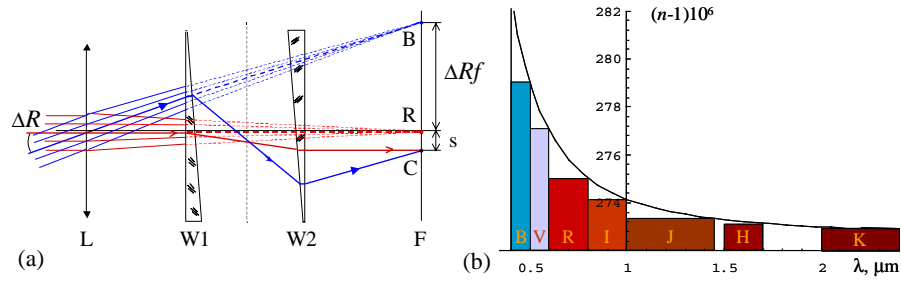

Fig. 2. Schematic layout of the linear ADC and its function (a); refractivity of air at different spectral bands (b).

Table 1. Atmospheric dispersion ΔR at a zenith angle z=45° compared with Airy disk radius r_A of a 42-m ELT.

Spectral band	B	V	R	I	J	H	K
λ range, μm	0.391-0.489	0.505-0.595	0.59-0.81	0.78-1.02	1.06-1.44	1.50-1.70	1.96-2.44
ΔR, milliarcsec	730	290	350	190	110	23	18
r_A, milliarcsec	2.7	3.3	4.2	5.4	7.2	9.6	13.2
Ratio $\Delta R / r_A$	270	88	83	35	15	2.4	1.4

The amount of dispersion introduced by the ADC is proportional to the axial distance between the two wedges, which makes it possible to match the effect of the ADC to a current value of atmospheric dispersion by moving one of the wedges along the optical axis. The linear ADC is especially advantageous for telescopes with an alt-azimuth mount because of the fixed direction of the atmospheric dispersion with respect to the telescope tube. The ADC preserves the direction of the chief ray, but displaces the image laterally (as well as the telescope optical axis) by an amount s, which can be approximately calculated as $s = d(n-1)\theta$, where d is the axial separation of the wedges with refractive index n and wedge angle θ. It becomes necessary to compensate for the optical axis shift s when re-directing light to a Nasmyth platform by a 45-deg beam splitter M4, see Fig. 1(b). In this case, one could translate the beam splitter along the telescope elevation axis by the same amount s so that the centre of the image stays fixed on the Nasmyth platform, which determines the position of the rotation axis for an instrument table used as a field de-rotator on the Nasmyth platform. The beam splitter displacement causes defocus of the image at the Nasmyth focus, which can be eliminated by adjusting the distance between the primary and the secondary mirrors (telescope refocusing) or by changing the height of the instrument table.

3. Optical design of the linear ADC

Table 1 lists values of atmospheric dispersion ΔR in seven spectral bands (from B to K) and the Airy disk radius for a 42-m ELT. The Airy disk radius is comparable with the full width at half maximum of the point-spread function (PSF). We can see that the amount of atmospheric dispersion is 270 times larger than the Airy disk radius in the B band and about 80 times larger for V and R bands. It is evident that increasing the size of the telescope aperture and using AO correction reduces the width of the PSF, which, in turn, makes the atmospheric dispersion correction more challenging.

For atmospheric model we assumed conditions corresponding to a site at Observatorio del Roque de los Muchachos, La Palma: 2560 meter elevation, 0°C temperature, 675 millibar pressure, 30%, relative humidity, and 32 degree latitude. For our ADC performance analysis

we used the atmospheric dispersion model in Zemax software. A maximum zenith distance of 50 degrees has been assumed.

The goal of the optical design for the linear ADC is to preserve the intrinsic quality of the 42-m ELT optical system within a 1-arcmin field of view. Inserting an ADC into f/15.2 converging beam degrades image quality of the Gregorian system, however if the secondary mirror is a deformable mirror, one could correct for variable coma and astigmatism introduced by the ADC wedges. Spherical aberration is negligible due to a relatively small converging angle of the beam and moderate thickness of the wedges.

An optical layout of the linear ADC is presented in Fig. 1(b). The first wedge W1 travels vertically above the instrument table at the Nasmyth focus. An unobstructed path for a 3 arcmin field requires a 0.75 m optical diameter for W1. The second wedge W2 is positioned 1 m away from the focus, hence its diameter is smaller (0.72 m). In order to avoid flexure of wedges due to their own weight, we choose a central thickness of 40 mm. We opted for a relatively large wedge angle of 3 degrees to reduce the travel range of W1. For correction of atmospheric dispersion in the V band we selected flint glass F5 from the Schott catalog. This type of glass has good internal transmission in the VRIJ bands.

Figure 3(a) shows optical performance (Strehl ratio vs field angle in VRIJ bands) achievable with wedges made of F5 glass over 1 arcmin field; atmospheric turbulence is not taken into account. It is obvious that this type of flint glass matches atmospheric dispersion well in the V band only. Correction in other spectral bands is less efficient due to some residual secondary spectrum.
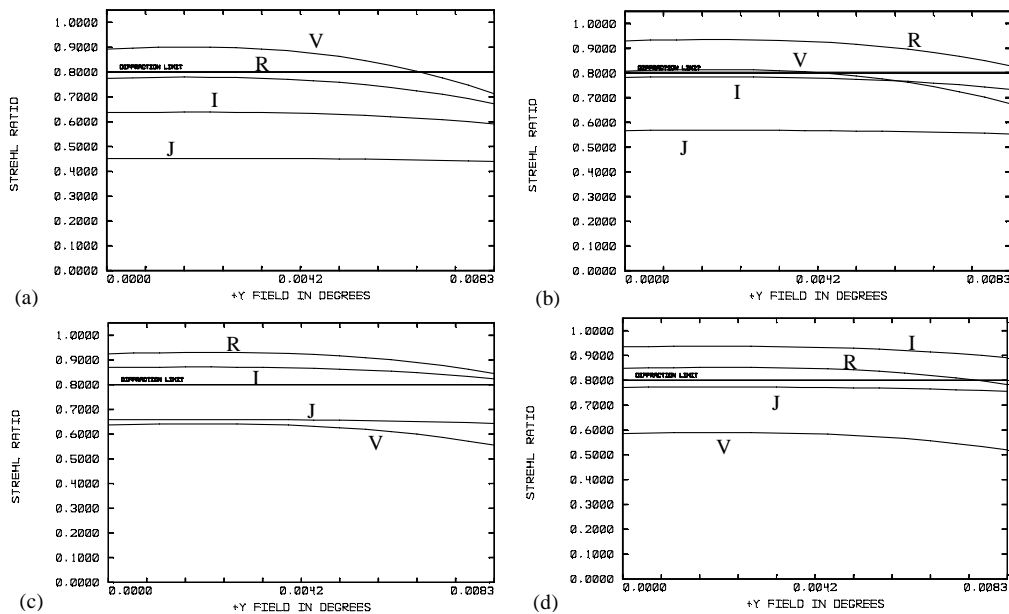

Fig. 3. Atmospheric dispersion correction at 50 deg off-zenith using wedges made of F5 glass (a), SF5 glass (b), SF14 glass (c), and SF57 glass (d). The image degrading effects of atmospheric turbulence are not included.

Choosing SF5 glass helps to reach diffraction-limited correction in the R band and reduces secondary spectrum in the I and J bands, while slightly worsening performance in the V band. One could further improve performance in the I and J bands by selecting SF14 glass, while SF57 glass is particularly good for optimal performance in the R, I and J bands, see Fig. 3(c) and Fig. 3(d), which is most probable wavelength range for AO systems to be used on ELTs.

An example of a telescope adjustment look-up table for different spectral bands is presented in Table 2. Considering the 50-deg zenith distance allows us to see the typical

values of adjustment parameters under the most challenging operation conditions. The coefficient A_6 and A_7 are given for Zernike standard circular polynomials, namely for terms $Z_6(\rho, \varphi) = 6^{1/2} A_6 \rho^2 \cos 2\varphi$ and $Z_7(\rho, \varphi) = 8^{1/2} A_7 (3\rho^3 - 2\rho) \sin\varphi$, where ρ and φ are polar coordinates in the pupil. The coefficients A_6 and A_7 represent the RMS value of astigmatism and coma respectively. These terms should be applied on the deformable secondary to compensate the intrinsic aberrations caused by the linear ADC. The wedge separation d and lateral image displacement s (to be compensated by translating the beamsplitter M4) are also given. The telescope optical system was optimized for a 1-arcmin full field of view required for a single-conjugate AO.

Table 2. Telescope system adjustment for 50-deg off-zenith: secondary mirror deformation (RMS value in μm), wedge separation and beamsplitter translation to retain the image position at Nasmyth focus (units are mm).

Band	F5				SF5				SF57			
	A_6	A_7	d	s	A_6	A_7	d	s	A_6	A_7	d	s
V	2.1	0.8	1845	65	1.8	0.7	1397	56	1.4	0.5	815	47
R	2.0	0.7	1849	64	1.8	0.7	1423	57	1.4	0.5	865	47
I	1.8	0.7	1680	57	1.6	0.6	1349	52	1.4	0.5	863	46
J	1.2	0.5	1397	38	1.2	0.5	979	38	1.1	0.4	713	38

Figure 4 depicts correction of atmospheric dispersion on axis for the first case (F5 glass). In spite of the fact that RMS spot size is well within the Airy disk, we do not achieve diffraction-limited image quality in all spectral bands when considering the polychromatic wavefront error. This error is larger than wavefront error calculated for a single wavelength within that spectral band. The residual dispersion makes the PSF elongated in a vertical direction reducing Strehl ratios below the 0.8 level in the RIJ bands owing to a mismatch between the dispersion of F5 glass and that of the Earth's atmosphere. One could optimize the ADC performance for the central spectral band of a specific wavelength range, as illustrated in Fig. 3(b) for the R band.
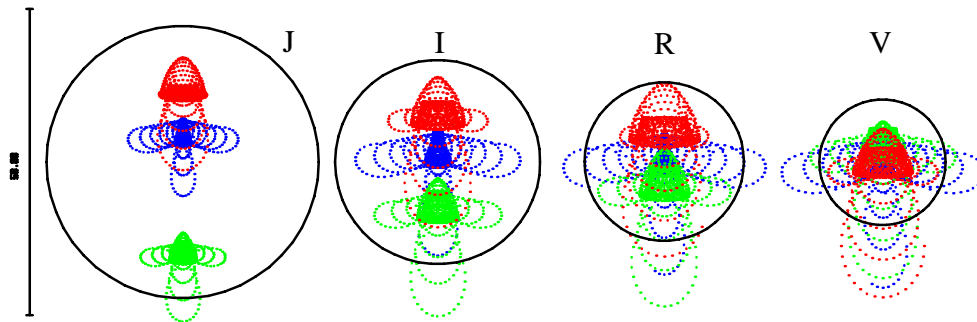

Fig. 4. Residual dispersion at the field center after correction with a linear ADC using F5 glass wedges in the V, R, I, and J bands at 50-deg zenith distance, for corresponding Strehl ratios see Fig. 3(a). Spot diagram plot scale is 50 μm.

Selecting a glass of high refractive index helps reducing either wedge motion range or wedge angle. As can be seen from Table 2, for SF57 glass (*n*=1.8) the maximum wedge separation is less than 1 m. From a mechanical point of view, the extensive motion range required for the wedge in the linear ADC might be practically more challenging to implement than rotation of compound prisms in alternative ADC systems. However, the Amici prisms require larger wedge angles and cannot be used near the telescope focus, whereas a linear ADC can operate in vicinity of the focus, which helps to minimize its optical diameter.

It is worth noting that telescope refocusing can be achieved by applying a defocus term $Z_4 = 2^{1/2} A_4 (2\rho^2 - 1)$ on the deformable secondary mirror, but it is preferable to save a mirror stroke for AO correction and maintain the image position simply by adjusting the distance

between the primary and the secondary mirrors. Refocusing the telescope by these methods inevitably leads to changes in plate scale at the Nasmyth focus. This effect is not negligible for observing over an extensive range of zenith distances. Compensating a 50-mm focus shift by adjusting the shape or position of the secondary mirror results in the rescaling of the image with a radial displacement of 0.03 arcsec at the field edge (0.5 arcmin from the center). It is desirable to retain the plate scale of the telescope over long exposures, however it might be difficult to run the AO system for such a long time, especially at large zenith distances, and turbulence-induced image-blur could surpass the effect of the image rescaling.

In principle to keep the plate scale constant when refocusing the telescope with M2, one could adjust the shape of M1 and position or shape of M2 simultaneously. Since M1 is segmented and controlled by edge sensors (not sensitive to curvature changes) a dedicated wavefront sensor will be needed for controlling the M1 curvature, and this could be done in combination with control of either curvature or displacement of M2 in such a way that the magnification (plate scale) is always kept constant.

Another technical issue worth mentioning here is the image quality of LGSs used in a wavefront sensing system. The Sodium LGS are generated in the Sodium layer at about 90 km altitude above the ground. The monochromatic light of LGSs (λ=0.589 microns) is not affected by atmospheric dispersion, and therefore the apparent position of the LGSs on the sky remains fixed with respect to the line of sight of the telescope.

The image quality of LGSs is mainly degraded by their proximity to the telescope aperture, and it is well known that apart from large defocus, LGSs suffer from spherical aberration and field aberrations, such as coma and astigmatism, see Fig. 5. For Gregorian systems, the aberration coma is a dominant factor producing about 0.7-micron RMS wavefront error for a LGS at 1.5 arcmin off-axis, the coma scales linearly with the field angle and varies with telescope elevation, Fig 5(b). Comparing Figs. 5(a) and 5(b) for the case when observing at 1-deg zenith distance, we conclude that the contribution of the ADC to the aberrated images of LGSs is negligible. Therefore regardless whether LGS light goes through the ADC or not, we still have to compensate the larger amount of coma in the LGS beams, and its variability makes wavefront sensing is challenging.
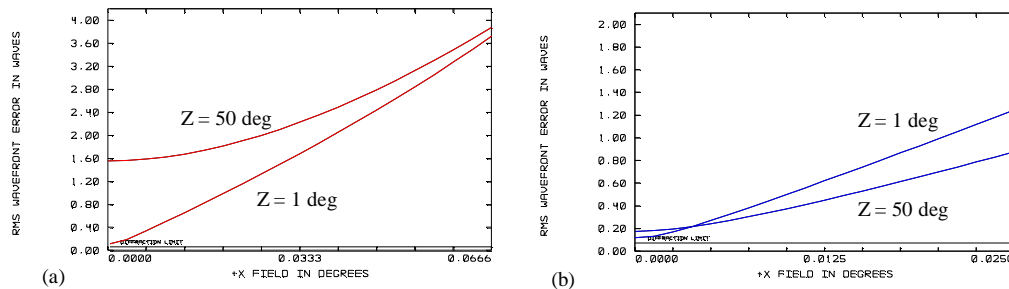

Fig. 5. The image quality of LGSs after reflection from M2 (a) and after passing the ADC (b). Atmospheric dispersion correction within 1 arcmin field with wedges made of F5 glass at zenith distance of 1 and 50 degrees. Note the difference in scale for cases (a) and (b).

The main reason to make ADC as big as possible, 0.75 m diameter seems feasible, is not only to have an option of passing LGS beams through, but more importantly to maximize available field of view for science and observations requiring larger fields, since we need the ADC not only for narrow-field adaptive optics mode. In that respect, it is quite likely that one of the first operation modes of future telescopes will include ground layer correcting adaptive optics, which requires wider separation of LGSs on the sky. In this mode, marginal LGSs are positioned about 3-4 arcmin off axis, and we cannot propagate LGS beams through the ADC (1.5 m diameter is not feasible). One of the possible ways to avoid this problem is to pass the central LGSs trough folding flat M4, see Fig. 1, and the marginal LGSs near the edge of M4 without crossing it. In this case, the Zernike terms introduced on M2 to compensate intrinsic

aberrations of the ADC, the coma and astigmatism, add some additional aberrations to LGS beams. Figure 5(a) shows that for the central LGS this wavefront error reaches its maximum (0.8-micron RMS) when observing at the 50-deg zenith distance. One the other hand, the field aberrations of the marginal LGSs (4-arcmin off axis), due to their finite distance, amount to 2.2 microns RMS error, which is a bigger effect than the effect introduced by M2. The total wavefront error might be corrected by a zoom-like lens system possibly featuring wedges.

Conclusion

In this article, we have studied the benefit of using the linear ADC on ELTs equipped with AO systems. In the course of this analysis, the following points have been under scrutiny: the optical design of the ADC and its performance for a 42-m ELT. Four potential designs for a Nasmyth focus have been presented and assessed. These various designs are tuned for different spectral bands. All of these designs provide diffraction-limited image quality over a 1-arcmin field. The use of a deformable mirror to correct the intrinsic aberrations of the ADC is of particular importance. Atmospheric dispersion compensation over a broader wavelength range is not practical due to chromatic path length error, which undermines the AO correction. This effect is particular harmful for the PSF background level on ELTs and should be taken into account along with the dispersion displacement error [27]. The latter chromatic effect will be dominant at large zenith distances and will ultimately limit the AO performance.